Structures of the Noncovalent Complexes of Human and Bovine Prothrombin Fragment 2 with Human PPACK–Thrombin[†,‡]

Raghuvir K. Arni,[§] Kaillathe Padmanabhan, K. P. Padmanabhan, Tswei-Ping Wu, and A. Tulinsky[*]

Department of Chemistry, Michigan State University, East Lansing, Michigan 48824-1322

Received December 14, 1992; Revised Manuscript Received March 2, 1993

ABSTRACT: Both human and bovine prothrombin fragment 2 (the second kringle) have been cocrystallized separately with human PPACK (D-Phe-Pro-Arg)–thrombin, and the structures of these noncovalent complexes have been determined and refined (R = 0.155 and 0.157, respectively) at 3.3-Å resolution using X-ray crystallographic methods. The kringles interact with thrombin at a site that has previously been proposed to be the heparin binding region. The latter is a highly electropositive surface near the C-terminal helix of thrombin abundant in arginine and lysine residues. These form salt bridges with acidic side chains of kringle 2. Somewhat unexpectedly, the negative groups of the kringle correspond to an enlarged anionic center of the lysine binding site of lysine binding kringles such as plasminogens K1 and K4 and TPA K2. The anionic motif is DGDEE in prothrombin kringle 2. The corresponding cationic center of the lysine binding site region has an unfavorable Arg70Asp substitution, but Lys35 is conserved. However, the folding of fragment 2 is different from that of prothrombin kringle 1 and other kringles: the second outer loop possesses a distorted two-turn helix, and the hairpin β-turn of the second inner loop pivots at Val64 and Asp70 by 60°. Lys35 is located on a turn of the helix, which causes it to project into solvent space in the fragment 2–thrombin complex, thereby devastating any vestige of the cationic center of the lysine binding site. Since fragment 2 has not been reported to bind lysine, it most likely has a different inherent folding conformation for the second outer loop, as has also been observed to be the case with TPA K2 and the urokinase kringle. The movement of the Val64–Asp70 β-turn is most likely a conformational change accompanying complexation, *which reveals a new heretofore unsuspected flexibility in kringles*. The fragment 2–thrombin complex is only the second cassette module–catalytic domain structure to be determined for a multidomain blood protein and only the third domain–domain interaction to be described among such proteins, the others being factor Xa without a Gla domain and Ca^{2+} prothrombin fragment 1 with a Gla domain and a kringle.

The N-terminal region of prothrombin preceding prethrombin 2, the immediate inactive precursor of the α-thrombin catalytic domain, can be divided into three segments with molecular masses of about 7000, 16 000, and 15 000 Da, respectively (Figure 1). Through a series of posttranslational modifications the ten glutamic acids in the first 33 residues of the prothrombin molecule are carboxylated to Gla[1] residues by a vitamin K dependent carboxylase, and since the region appears to be autonomous and is highly homologous (65%) to the N-terminal peptides of factors VII, IX, and X and the proteins designated C, S, and Z, it has become known as the Gla domain. The Gla domain is essentially unfolded in the absence of Ca^{2+} ions (Tulinsky et al., 1988b) but can bind seven Ca^{2+} ions in a linear, polymeric array to produce a structure that adheres to membrane and phospholipid surfaces (Soriano-Garcia et al., 1992). The Gla domain, the trailing tetradecapeptide disulfide loop, and the three-disulfide, triple loop kringle 1 module constitute prothrombin fragment 1 (Figure 1). The kringles of fragment 1 and fragment 2 are homologous, and on the basis of the 40% identity between the two (Magnusson et al., 1975) (Figure 1), it has been suggested that a partial gene duplication may have occurred during the evolution of prothrombin (Hewett-Emmett et al., 1974; Elion et al., 1986). Prothrombin F1 is obtained by proteolytic cleavage of prothrombin at Arg156 by thrombin.

Kringles are a common motif occurring in many proteins involved in blood coagulation and fibrinolysis (Patthy, 1985; McLean et al., 1987; Tulinsky, 1991). The function of some is to bind to fibrin (Lerch et al., 1980; Vali & Patthy, 1984), and although the function of the Gla domain of F1 is to bind to phospholipid (Stenflo, 1974; Baja et al., 1975; Nelsestuen, 1976), the F1 kringle has no known function. The ten Gla residues in prothrombin F1 can bind Ca^{2+} ions, whereupon there is a fluorescence quenching event implying a conformational change (Nelsestuen, 1976; Prendergast & Mann, 1977). The change has also been observed by circular dichroism (Bloom & Mann, 1978) and has since been established to be a folding transition by crystallographic studies of bovine F1 in the absence (Park & Tulinsky, 1986; Tulinsky et al., 1988b; Seshadri et al., 1991) and in the presence of Ca^{2+} (Soriano-Garcia et al., 1992) or Sr^{2+} ions (unpublished results of this laboratory). Calcium ion binding and the associated conformational change are essential requirements for the binding of prothrombin and F1 to membranes that contain acidic phospholipids (Dombrose et al., 1979). The membrane binding capability in the presence of Ca^{2+} ions is thought to be important for the effective presentation of prothrombin as a substrate and for its subsequent activation

[†] This work was supported by NIH Grants HL 25942 and HL 43229.

[‡] The coordinates of both the HF2- and BF2-thrombin structures have been deposited in the Brookhaven Protein Data Bank under Accession Numbers 1HPQ and 1HPP, respectively.

[*] To whom correspondence should be addressed.

[§] Present address: Department of Physics, UNESP-IBILCE, Cx.P. 136, CEP 15 054-000, Sao Jose Do Rio Preto-SP, Brazil.

[1] Abbreviations: Gla, γ-carboxyglutamic acid; Gla domain, prothrombin$_{1-48}$; kringle, prothrombin$_{66-144}$ or facsimile also designated by a K; fragment 1 (F1), prothrombin$_{1-156}$; fragment 2 (F2), prothrombin$_{157-274}$; TPA, tissue-type plasminogen activator; ACA, ϵ-aminocaproic acid; BF2, bovine F2; HF2, human F2; PPACK, D-Phe-Pro-Arg chloromethyl ketone; hirugen, hirudin$_{53-64}$.

0006-2960/93/0432-4727$04.00/0

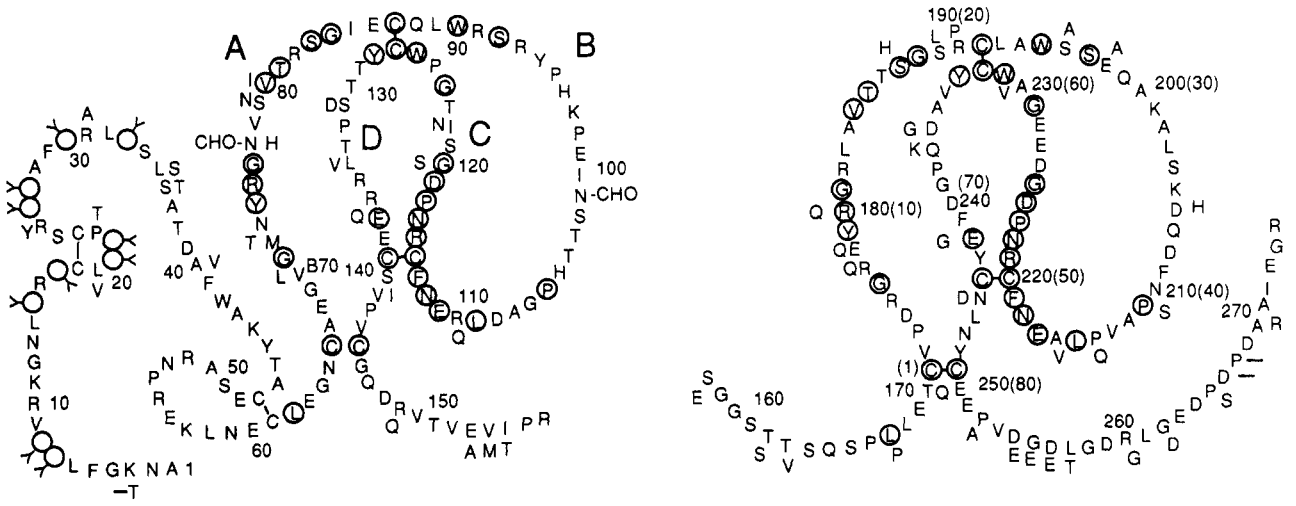

FIGURE 1: Sequences of bovine prothrombin fragment 1 (left) and fragment 2 (right). Alternate residues of human counterparts are indicated to the side of bovine sequences. Conserved residues between F1 and F2 in bovine are circled; Gla residues are designated by open circles and a Y; deletions are indicated with a hyphen; loops of kringles are designated A, B, C, and D; CHO is the site of carbohydrate attachment; sequential numbering of a single kringle beginning with the first disulfide is given for F2 in parentheses; numbers of 301 or greater in the text correspond to F2 beginning with the first disulfide; the other numbering in the figure corresponds to prothrombin.

to thrombin, in the physiologic prothrombinase complex (Nesheim et al., 1980; Mann, 1987), which additionally encompasses the enyme factor Xa and a nonenzyme membrane-bound cofactor (factor Va).

The kringle structure was the first blood protein domain to be determined by X-ray crystallography as the kringle of fragment 1 (Park & Tulinsky, 1986), where the 35 N-terminal residues of the Gla domain (75%) are flexibly disordered in the crystal structure. The folding of the kringle sequence appears to be based upon close van der Waals contacts between the inner-loop disulfides (Cys87–Cys127; Cys115–Cys139) (Figure 1). The sulfur cluster is buried in the interior of the folded structure and is inaccessible to solvent (Seshadri et al., 1991). Several other kringle structures have now been determined crystallographically: plasminogen K1 (unpublished results of this laboratory), plasminogen K4 (Mulichak et al., 1991), and TPA K2 (de Vos et al., 1992). The latter three bind to fibrin and lysine, ω-aminocarboxylic acids in general, and ACA in particular.

The residues in positions Asp57 and Arg71 of plasminogens K1 and K4 (numbering beginning at Cys1)[2] have been implicated as ionic centers (Trexler et al., 1982), while Arg32 and Arg34 have been shown to be essential for the fibrin binding affinity of plasminogen K1 (Vali & Patthy, 1984). The lysine binding subsite of fibrin binding kringles was first described in three dimensions by modeling based on the folding and tertiary structure of K1 of fragment 1 (Tulinsky et al., 1988a). It was later confirmed by the structure determination of plasminogen K4 with ACA in the binding site (Wu et al., 1991). A zwitterionic ACA in an extended conformation lies between doubly charged anionic and cationic centers of K4 formed by Asp55/Asp57 and Lys35/Arg71.

The second kringle and interkringle peptide regions of prothrombin correspond to prothrombin fragment 2 (Figure 1). This kringle is identical in loop lengths with kringle 1 of prothrombin and has been said to bind Ca^{2+} ions and to the heavy chain of factor Va (Esmon & Jackson, 1974; Bajaj et al., 1975). It also associates with α-thrombin, possessing a K_d in the nanomolar range (Myrmel et al., 1976) where thrombin most likely mimics prethrombin 2 in the complex producing a prethrombin 1-like fragment (F2 linked to prethrombin 2). The binding of F2 partially protects thrombin from inactivation by antithrombin III (Walker & Esmon, 1979), which is specific for thrombin since factor Xa is not protected in a similar manner. Prothrombin F2 also acts as a competitive inhibitor of protein C activation (Jakubowski et al., 1986), and BF2 enhances esterolytic activity of both human and bovine α-thrombins, but HF2 does not (Myrmel et al., 1976).

Thrombin is a glycoprotein that functions as a serine protease when it is generated from prothrombin in the final events of blood coagulation (Mann, 1987). The serine proteinase module is a common catalytic domain of blood proteins (thrombin, factors IXa and Xa, urokinase, TPA, plasmin, protein C), which are about 50% homologous among themselves, and simpler proteases like trypsin and chymotrypsin. Thrombin converts fibrinogen into clottable fibrin by exhibiting a specificity largely attributable to an anion binding exo site distinct from the catalytic site (Fenton, 1986). The fibrinogen recognition site has been shown to consist of a highly electropositive region comprised of the 70–80 loop on the surface of the molecule (Bode et al., 1989; Rydel et al., 1991; Skrzypczak-Jankun et al., 1991; Qiu et al., 1992). Another comparably charged positive surface patch, including about ten Arg/Lys/His residues, occurs near the C-terminal helix of the B-chain of thrombin (Bode et al., 1992; Karshikov et al., 1992), which has been presumed to be the heparin binding site of the molecule, consistent with it being an exo site that is different from the fibrinogen recognition site (Church et al., 1989).

We report here the crystallographic structures of HF2 and BF2 complexed with human α-thrombin inhibited by PPACK. Although crystals of the complex diffract X-rays to only about 3.3-Å resolution, the binding interaction between F2 and thrombin in the structure of the complex is clear and occurs in a region reported to be the putative heparin binding site (Church et al., 1989; Bode et al., 1992; Karshikov et al., 1992). The folding of the F2 kringle differs significantly from that of the kringle of F1 and other kringles of known structure with similar loop sizes and is consistent with at least a partial conformational change in F2 that appears to optimize the

[2] The numbering in different kringles may vary somewhat depending on the sizes of the various loops; thrombin numbering is based on topological similarities with chymotrypsinogen with insertions designated by letters as described by Bode et al. (1992).

Table I: Unit Cell Dimensions of HF2– and BF2–Thrombin

	HF2–thrombin	BF2–thrombin
cell constants (Å)		
a	123.6	122.7
b	123.6	122.7
c	101.1	103.7
V_m (Å^3/Da)	3.76	3.80
solvent content (%)	60	60

binding interaction with thrombin. The binding interaction is principally ionic with an aromatic stacking component; the former involves an enlarged anionic center of the lysine binding site of lysine-binding kringles (Tulinsky et al., 1988a) and a group of arginine residues located near the C-terminal helix of thrombin (Rydel et al., 1990; Bode et al., 1992). The resulting two-domain arrangement is most likely related to the protection afforded to thrombin against antithrombin III inactivation. The complexes of HF2 and BF2 with thrombin are practically the same since the nonconserved residues between the kringle species do not generally participate in and are not important for the binding association.

EXPERIMENTAL PROCEDURES

Human PPACK–α-thrombin was used in the crystallization experiments to ensure against autolysis. It was supplied by Dr. John W. Fenton II as 1-mL samples of frozen solution at a protein concentration of 0.94 mg/mL in 0.75 M NaCl. PPACK–thrombin was first diluted with an equal amount of 0.1 M sodium phosphate buffer (pH 7.3) and concentrated to 7 mg/mL using a Centricon-10 miniconcentrator in a refrigerated centrifuge. An approximately 10% molar excess of HF2, a gift of Dr. Craig M. Jackson, necessary to form a 1:1 complex was added to the concentrated protein solution. Crystals were grown by hanging and sitting drop vapor diffusion methods. The initial crystallization conditions of the complex were ascertained by an incomplete factorial search (Carter & Carter, 1979). Typically, 2-μL drops of the protein were used for each individual trial to which an equal volume of precipitant was added. The factorial solution with 0.1 M ammonium sulfate, 30% PEG 8000, and 0.1 M citrate buffer at pH 5.5 yielded small crystals in 2 days. Refinement of the crystallization conditions was accomplished by macroseeding. Drops were preequilibrated for 24 h prior to seeding. The crystal of HF2–thrombin used for intensity data collection (1.4 × 0.2 × 0.1 mm) was grown from a sitting drop with a PEG concentration of 16%.

The complex between BF2, supplied by Dr. K. G. Mann, and human PPACK–α-thrombin was made in the same way as that of the HF2 complex. In this case, however, the crystals were grown from 0.2 M sodium potassium tartrate, 18% PEG 8000, and 0.1 M ADA, pH 6.5. The BF2–thrombin crystal used for the intensity data collection was a little smaller (1.0 × 0.25 × 0.1 mm). Both complexes belong to the tetragonal crystal class, space group $P4_12_12$, with eight complexes per unit cell. Although the complexes are fairly isomorphous (Table I), the *c*-axis of BF2–thrombin is significantly larger (2.5%).

Three-dimensional X-ray diffraction data were collected at room temperature by utilizing a Siemens Xentronics area detector and graphite monochromated Cu Kα radiation generated by a Rigaku RU200 X-ray generator operating at 7.5 kW. The crystal–detector distance was 13.0 cm, the detector swing angle was 5.0°, and the scan range was 0.2° per frame; each frame was collected for 200 s, with diffraction extending to only 3.3-Å resolution for the HF2–thrombin and about 3.2 Å for the BF2 complex, even though the size of the crystals used was considerable. A 0.3-mm collimator was used that enabled collecting a second diffraction data set from the same crystal by translating the crystal along its long dimension to expose a fresh part of the crystal. Intensity data reduction was carried out using the XENGEN (Howard et al., 1987) suite of programs. A total of 62 904 observations were measured for the two translational settings of the BF2 complex, of which 11 368 were independent. After reflections with $I/\sigma(I) < 2$ were removed, 9115 unique reflections remained (70% observed; $R_{merge} = 0.052$). Half the reciprocal sphere was surveyed with the HF2–thrombin data set to confirm the crystal class (51 004 observations). The data of the two independent translational settings (~100 000 observations) were merged to a unique set with $R_{merge} = 0.084$. Since R_{merge} was only 0.069 for the first setting alone, the second crystal setting measurements, which appeared to be less accurate due to radiation-induced decay, were not used, giving 9195 reflections with $I/\sigma(I) > 2$ and $R_{merge} = 0.065$ for HF2–thrombin.

Crystals of BF2–thrombin were obtained first, so the description of the structure analysis to follow begins with these crystals for logical continuity. Patterson rotation/translation molecular replacement methods were used to solve the phase problem and the structure of the BF2–thrombin complex. The atomic coordinates of human α-thrombin complexed with hirugen (Skrzypczak-Jankun et al., 1991), stripped of solvent and hirugen, were employed as a search model for BF2–thrombin. The rotation search was initially carried out with MERLOT (Fitzgerald, 1988) and data between 10.0–4.0-Å resolution and $|F| > 3\sigma(|F|)$. A single solution was obtained with a height of 18 rms above the average (next highest peak 5.4 rms). The rotation search was repeated with the program X-PLOR (Brunger, 1990a), which gave the same solution but with a peak of 7.5 (4.3 rms above mean); surprisingly, the next highest peak was at a height of 7.2. However, Patterson correlation refinement (Brunger, 1990b) confirmed the single, outstanding MERLOT solution (correlation coefficient = 0.09, next highest = 0.03).

Translation searches were conducted in both enantiomorphic space groups ($P4_12_12$ and $P4_32_12$) also using X-PLOR. A solution was obtained in the latter space group of 4.7 rms above the mean, while its enantiomorph produced a solution that was 16.9 rms above the mean with a correlation coefficient of 0.44 (0.29 next highest). Rigid body refinement of the $P4_12_12$ solution reduced the crystallographic residual from 0.41 to 0.37.

Initial refinement was carried out using restrained least-squares methods employing the program PROFFT (Finzel, 1987) with the structure of α-thrombin only and diffraction data in the 7.0–3.3-Å range. After 21 cycles, the refinement converged to a crystallographic *R*-value of 0.27. At this stage, $(2F_o - F_c)$ and $(F_o - F_c)$ maps were computed. The electron density maps clearly indicated the presence of PPACK in the active site and the position of the kringle of BF2. However, due to the lack of complete continuity in the electron density, the atomic model of the kringle of F1 (Tulinsky et al., 1988b) could not be fitted unambiguously to the maps. Thus, only fragments of the main chain were built into the electron density, which were improved upon in subsequent rounds of refinement by both restrained least-squares and simulated annealing methods (Brunger et al., 1987). After 125 cycles of refinement, the residual was reduced to 0.157 for data with $|F| > 2\sigma(|F|)$ between 10.0 and 3.3-Å resolution (9115 reflections).

Table II: Root Mean Square Deviations from Ideality, Target Restraints, and *R*-Factor Statistics of HF2–Thrombin and BF2–Thrombin

	rms deviation		
	HF2–thrombin	BF2–thrombin	target σ
distance restraint information (Å)			
bond distance	0.020	0.012	0.02
angle distance	0.059	0.049	0.04
planar 1–4 distance	0.066	0.059	0.06
plane restraint	0.01	0.01	0.02
chiral center restraints (Å^3)	0.135	0.161	0.150
nonbonded contact restraints (Å)			
single-torsion contact	0.25	0.25	0.55
multiple-torsion contact	0.30	0.30	0.55
possible (X–Y) hydrogen bond	0.30	0.30	0.55
conformational torsion angles (deg)			
planar	2	2	3
staggered	27	29	25
orthonormal	34	31	30
thermal parameter restraints (Å^2)			
main-chain bond	0.6	0.7	1.0
main-chain angle	1.1	1.3	1.5
side-chain bond	1.2	1.4	2.0
side-chain angle	1.9	2.4	2.5
av bond angle (deg)	116.8	116.8	
rms deviation [av angle (deg)]	3.7	3.4	
diffraction pattern			
HF2–thrombin $\sigma\|F_o\| = A + B[\sin(\theta/\lambda - (1/6)]$	$A = 36$	$B = -240$	$\langle\|\|F_o\| - \|F_c\|\|\rangle = 93$
BF2–thrombin $\sigma\|F_o\| = A + B[\sin(\theta/\lambda) - (1/6)]$	$A = 34$	$B = -275$	$\langle\|\|F_o\| - \|F_c\|\|\rangle = 103$

					R-value	
	d_{min} (Å)	no. of reflections	$\langle\|\|F_o\| - F_c\|\|\rangle$	$\sigma(\|F\|)$	shell	sphere
HF2–thrombin	6.5	1169	146	60	0.219	0.219
	5.3	1281	110	55	0.197	0.208
	4.6	1410	89	51	0.131	0.178
	4.2	1233	84	48	0.122	0.164
	3.9	1168	82	46	0.135	0.159
	3.6	1392	76	43	0.138	0.155
	3.3	1542	72	41	0.157	0.155
BF2–thrombin	6.5	1178	157	61	0.220	0.220
	5.3	1297	120	56	0.196	0.208
	4.6	1411	101	51	0.136	0.180
	4.2	1227	93	48	0.124	0.166
	3.9	1227	90	45	0.138	0.161
	3.6	1567	83	43	0.142	0.157
	3.3	1208	78	40	0.154	0.157

The coordinates of thrombin from the BF2–thrombin refinement were used for the solution of the structure of HF2–thrombin that began with a rigid-body refinement, which reduced the *R*-value from 0.43 to 0.33. At this stage, the coordinates of BF2 of the BF2–thrombin complex, with the nonconserved residues changed to Gly or Ala, were employed for a rigid-body refinement with the previously determined position and orientation of PPACK–thrombin. The residual of the combined rigid-body refinement started at 0.39 but reduced to 0.28. Nine cycles of restrained least-squares refinement lowered the *R*-factor further to 0.215. The resulting electron density maps of HF2–thrombin permitted the unambiguous building of the nonconserved residues between the human and bovine kringles into the $(2F_o - F_c)$ map. The refinement converged after 27 additional cycles of refinement at $R = 0.155$, also for the 10.0–3.3-Å resolution range.

The BF2–thrombin model consists of 2961 atoms and 120 solvent water molecules. There was no electron density for either the 14-residue interkringle or the 23-residue (25 for bovine) C-terminal kringle–catalytic domain connecting peptide. This extensive disorder, consisting of about 10% of the complex, is most likely the underlying cause for the relatively poor diffraction quality of the crystals. A similar disorder, but of shorter interkringle peptides, was observed in the plasminogen kringle 4 crystal structures (Mulichak et al., 1991; Wu et al., 1991). The solvent sites were chosen only if the highest density persisted in the electron density maps throughout the last few rounds of refinement. No attempt was made to locate further solvent molecules even through the solvent contribution appears to still be significant in the more accurately measured low-order diffraction data. This can be seen from the low-order shell residuals of Table II, which obviously still possess a significant solvent component to about 5.0-Å resolution. However, the better low-order data are offset somewhat by the protein structure being necessarily less accurate at an overall lower resolution, so that some of the difference electron density may also be attributable to this source. The 120 solvent water molecules included represent only about one-third that usually recorded for protein structures of this size at higher resolution. The HF2–thrombin structure, which includes 123 water molecules, also has disordered interkringle peptides. A summary of the stereochemical restraints, deviations of the geometrical structure, and diffraction data statistics is presented in Table II. The Ramachandran plots of HF2– and BF2–thrombin showed that both the kringle and the thrombin catalytic domain correspond well to allowed regions. The average *B*-value of thrombin for HF2–thrombin is 19 Å^2 and is 21 Å^2 for BF2–thrombin; however, those of HF2 and BF2 are considerably greater at about 40 Å^2. Reducing the occupancy of the kringle to 0.8 reduces the average *B*-value to about 30 Å^2. In view of the nanomolar binding constants of the complexes, a F2 occupancy of much less than unity is unlikely so that the

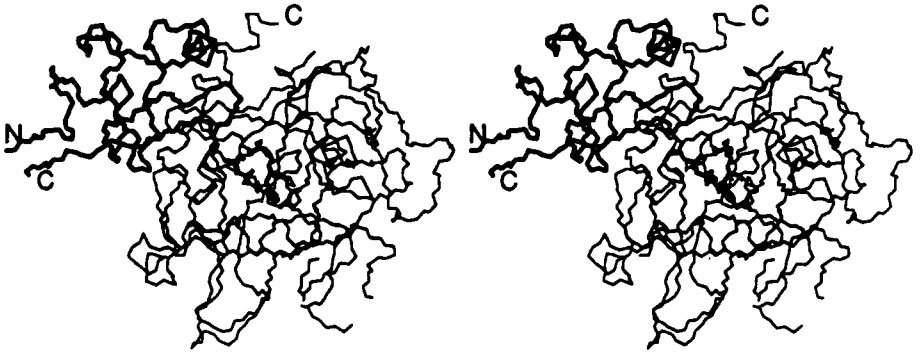

FIGURE 2: Stereoview of the CαCN structure of HF2–thrombin. The F2 kringle and the catalytic triad of thrombin are shown in bold; C- and N-termini of the kringle and the C-terminus of the thrombin B-chain are designated.

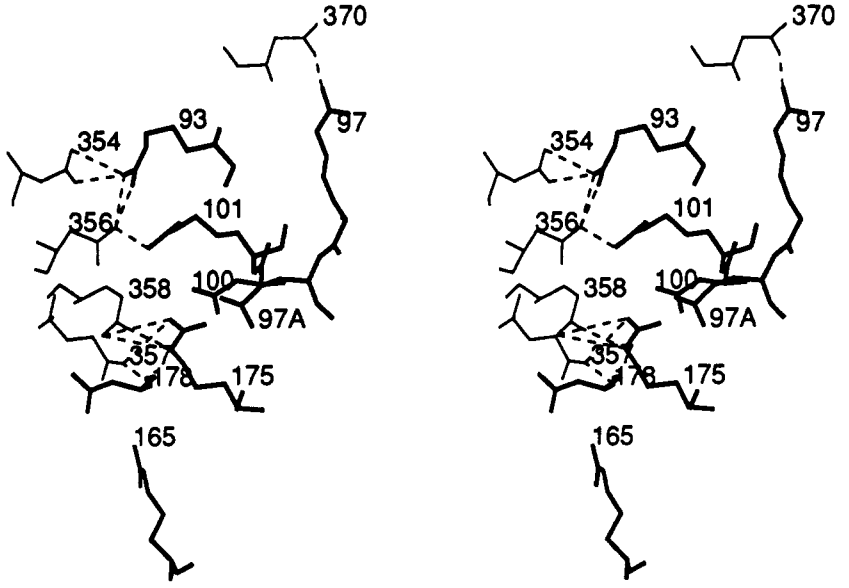

FIGURE 3: Stereoview of principal electrostatic interactions between HF2 and thrombin. Positively charged residues are shown in bold; ion pair interactions are designated with broken lines.

larger average *B*-value must be the result of a larger static disorder or lack of structural fidelity in the binding of the kringle. This is especially the case because of the disordered interkringle peptides, which are about half the size of the kringle itself.

RESULTS AND DISCUSSION

Kringle–Thrombin Interaction. Since the HF2- and BF2–thrombin complexes are very similar in structure, only the HF2–thrombin complex is described in detail; the BF2–thrombin complex will be referred to when significant differences are to be noted. The structure of the F2–thrombin complex is the second cassette module–catalytic domain structure to be determined for a multidomain blood protein, the other being a factor Xa structure lacking the Gla domain (Padmanabhan et al., 1993). Moreover, it is only the third double-domain structure to be described among such proteins, the other one being that of Ca^{2+} prothrombin fragment 1 (Gla domain and kringle 1) (Soriano-Garcia et al., 1992).

The main-chain polypeptide structure of the HF2–thrombin complex is shown in Figure 2, from which it will be seen that the fragment 2 kringle makes extensive contacts with thrombin. The kringle interacts at a thrombin site that has been proposed to be the putative heparin binding region (Church et al., 1989; Bode et al., 1992). The latter was confirmed to be a highly electropositive surface in electrostatic potential energy calculations (Karshikov et al., 1992) near the C-terminal helix of the B-chain of thrombin that is abundant in arginine and lysine residues. Not surprisingly then, these positively charged residues form salt bridges with acidic side chains of the kringle (Figure 3), some of which are hydrogen bonded (Table III). Somewhat unexpectedly, however, the negatively charged groups of the kringle correspond to an enlarged anionic center of the lysine binding site of lysine-binding kringles, such as kringles 1 and 4 of plasminogen and kringle 2 of TPA (Tulinsky et al., 1988b; Mulichak et al., 1991; Wu et al., 1991; Byeon & Llinas, 1991; de Vos et al., 1992). The anionic motif is

Table III: Kringle–Thrombin Ion Pairs, Hydrogen Bonds, and Close Contacts Less Than 4.0 Å Involving the Putative Heparin Site

thrombin	kringle	HF2 (Å)	BF2 (Å)	
Pro92O	Gly369N	3.0	3.3	H-bond?
Arg93NH2	Asp354OD1	3.1	3.4	ion pair
Arg93NH2	Asp354OD2	3.4	2.9	ion pair
Arg93NH1	Asp356OD1	2.4	2.9	H-bonded ion pair
Arg93NH2	Asp356OD1	3.4		ion pair
Arg93NH1	Tyr373OH	3.1	3.8	H-bond?
Tyr94O	Gly369N	3.8	3.8	
Trp96NE1	Pro368O	3.1	2.8	H-bond
Arg97NH2	Gly369O	3.6	3.7	
Arg97NE	Gly369O	3.1	3.3	
Arg97NH2	Asp370OD1	2.5	2.5	H-bond
Arg101NH2	Asp356OD1	3.6	3.3	ion pair
Arg175NE	Glu358OE1	3.9		
Arg175NE	Glu358OE2	3.8	3.5	ion pair
Arg175NH2	Glu357OE1		3.5	ion pair
Arg175NH2	Glu358OE2		3.8	ion pair
Asp178N	Glu357OE1	2.5	3.3	H-bond?

FIGURE 4: Stereoview of the supporting aromatic stacking interaction in HF2–thrombin. The kringle of the HF2 orientation is similar to that in Figure 2 with N- and C-termini designated.

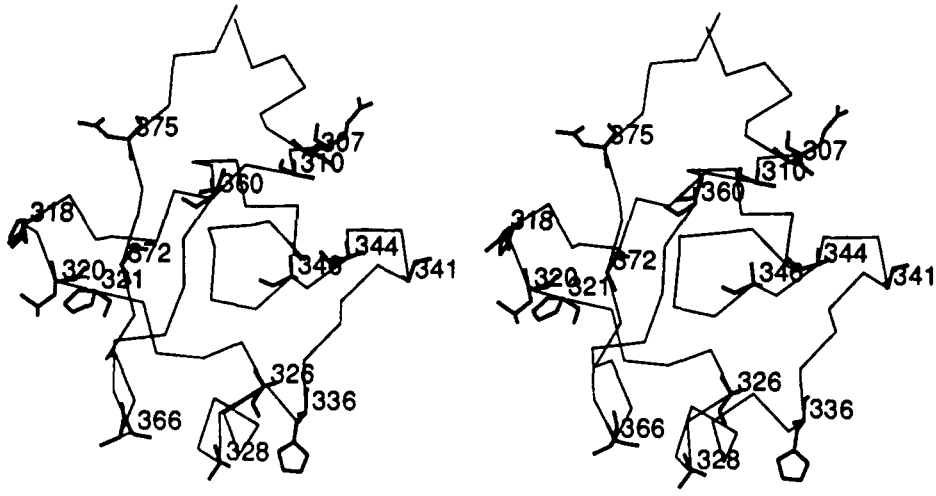

FIGURE 5: Stereoview of the Cα structure of HF2. The side chains indicated are those of HF2 at positions of nonconservation with BF2.

Asp-X-Asp in lysine-binding kringles but is AspGlyAspGluGlu in HF2 and BF2. The salt bridges are particularly intense between Arg93, Asp354, and Asp356 at one end of the interdomain contact and Arg175, Glu357, and Glu358 at the other end (Figure 3). The electrostatic interdomain interactions are additionally accompanied and apparently enhanced by an aromatic stacking component from each domain; the aromatics are located adjacent to each other in the complex (Figure 4). The aromatic residues of the kringle are the same ones that form the hydrophobic methylene binding trough of lysine-binding kringles (Mulichak et al., 1991; Wu et al., 1991; Byeon & Llinas, 1991; de Vos et al., 1992). The total number of contacts less than 4.0 Å between thrombin and HF2 in the interdomain interaction is about 102, while that of the BF2 complex is only 89. Although the sequence differences between HF2 and BF2 essentially do not occur in the interdomain region (Figure 5), the smaller number of contacts in BF2–thrombin would seem to suggest that other factors are operative in reducing the interaction between these molecules from different species. Thus, the lysine binding site region of F2 displays a different function from fibrin binding kringles and, moreover, is very likely not involved in binding to the heavy chain of membrane-bound factor Va in the formation of the prothrombinase complex (Esmon & Jackson, 1974; Nesheim et al., 1980; Mann, 1987). If the putative heparin binding site of thrombin becomes established to be authentic, the utilization of it by F2 will be yet another example of the multiple functional diversity displayed by the various binding regions of the thrombin molecule (Tulinsky & Qiu, 1992). Moreover, the utilization of the anionic center of lysine-binding kringles by F2 in binding to thrombin is an example of a similar diversity surfacing for kringles. Another is the recent report of heparin binding to the kringle of urokinase, where the electrical polarity of the anionic center between residues 52 and 60 is reversed by the presence of four arginine residues (Stephens et al., 1992).

There is another kringle–thrombin interaction in the crystal structure, where HF2 makes 37 contacts less than 4.0 Å with thrombin but BF2 only has 11. The difference here is directly related to the longer *c*-axis in the BF2–thrombin crystals (Table I). The most significant intermolecular contact in the region in both structures is an ion pair between Arg77A of the fibrinogen recognition exo site of thrombin and Glu358 of the kringle of a symmetry-related complex. The region from Thr317 to Leu320 is also involved but to a much lesser extent in BF2, which could be due to a His318Ser and a Leu320Ser substitution in the latter (Figure 1). In any case, all indications suggest that the region simply corresponds to an intermolecular contact between complexes, which is in agreement with fluorescence studies that show F2 and hirugen both bind independently to thrombin (Liu et al., 1991), and the loss of contacts in BF2–thrombin is directly related to the increase in the *c*-axis dimension in BF2–thrombin crystals. This part of thrombin also happens to correspond to the β-cleavage site (Arg77A) and to the thrombin binding region of the C-terminal of hirudin (Rydel et al., 1991) and hirugen (Skrzypczak-Jankun et al., 1991). The site is highly electropositive so that the intermolecular contact involving the anionic center of the kringle must also be driven to some extent by electrostatic forces.

The electrostatic forces producing the F2–thrombin interaction in the complex have been investigated by calculating the electrostatic potentials of HF2 and thrombin (BF2 results are very similar). The program DELPHI of the suite of Biosym

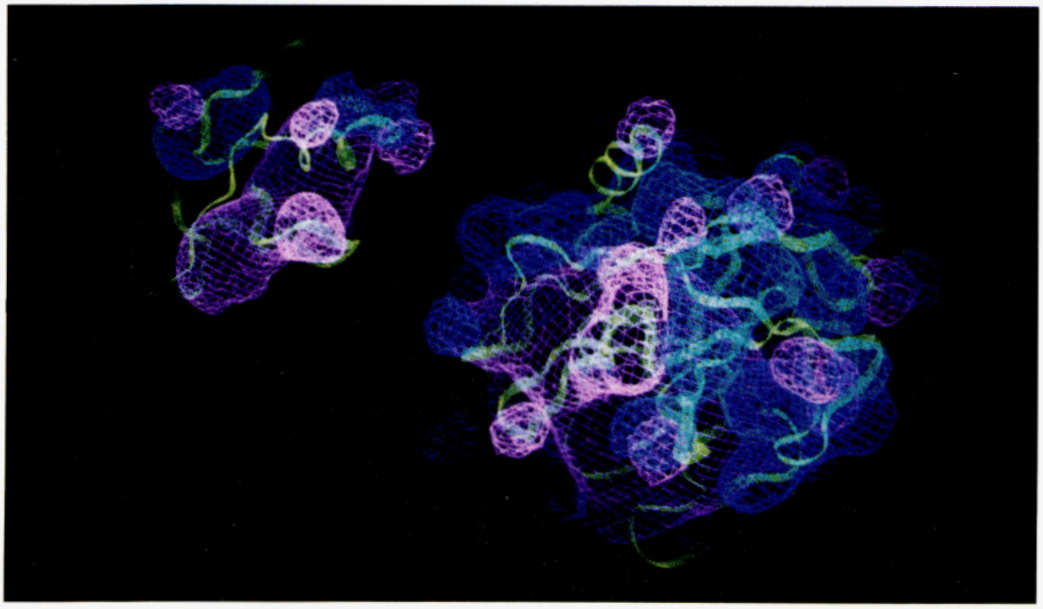

FIGURE 6: Separate electrostatic potentials of HF2 and thrombin. Contours are at 5.0 kT. Color coding: blue, positive; pink, negative; ribbon representation of folding, yellow. Orientations are the same as in Figure 2.

Table IV: Solvent Accessibilities of F2, Thrombin, and the Respective Complexes

	complex	thrombin	F2	thrombin/F2 covered	fraction of thrombin covered	fraction of F2 covered
				(A) HF2–Thrombin		
main chain (Å^2)	3610	2615	1298	303	0.12	0.24
side chain (Å^2)	11230	9457	3139	1366	0.14	0.44
all (Å^2)	14893	12072	4490	1669	0.14	0.37
				(B) BF2–Thrombin		
main chain (Å^2)	3407	2578	1120	291	0.11	0.26
side chain (Å^2)	11207	9335	3266	1394	0.15	0.43
all (Å^2)	14614	11913	4386	1685	0.14	0.38

programs was used for the calculation with 0.15 for the ionic strength of the solvent. The electrostatic potential superimposed on a ribbon representation of the folding of HF2 and thrombin is shown in Figure 6. The potentials of the kringle and thrombin have been calculated separately but are depicted in the same orientation as they occur in the intact complex. From Figure 6, it can be seen that the positive potential extending from the C-terminal helix is remarkably complementary to the negative potential recesses of the lysine binding-like anionic center of HF2. The electrostatic potential of the intact complex shows that the potential of the interface region between the two domains is essentially compensated and neutral.

The solvent accessibilities of F2, thrombin, and the respective complexes are compared in Table IV. The calculation was carried out by probing the surface with a sphere of 1.4-Å radius (Lee & Richards, 1971). From Table IV, it can be seen that a relatively exposed part of thrombin is involved in complex formation since both the main and side chains are covered equally in the complex. The same is not the case with the kringles where the side chains lose nearly twice the accessibility of the main chain. This appears to be related to the smaller globular structure of the kringle and its compact secondary structural β-strand components, which are generally buried. The fraction of surface covered is the same in both the HF2– and BF2–thrombin complexes, indicating that the increase in the *c*-axis unit cell dimension essentially results in lengthening the separation of the complexes in this direction and not from the separation of F2 and thrombin in the individual complexes.

Conformational Changes. The Cα structure of thrombin in HF2–thrombin and that of thrombin in the PPACK–thrombin complex (Bode et al., 1992) have been compared in order to ascertain structural changes accompanying complex formation. The structure of PPACK–thrombin used was that reported by Qiu et al. (1992), which, although at higher resolution, was measured and refined comparably to the F2–thrombin complexes; the PPACK–thrombin structure of Bode et al. (1992) was not used since a different refinement protocol was utilized and because it contains a very extended water structure. Using the former, the rms difference in positions is 0.7 Å; removing 35 differences $>1\sigma$ (about 13%) reduces this to 0.3 Å, which is within the error of the structure determination. Minor changes are observed in the conformations of two of the side groups in the interdomain region (Arg93 and Arg175); however, the guanidinium groups appear to be in positions similar to those of PPACK–thrombin. These, along with Arg101, are involved in the dominant interactions with the kringle module (Figure 3). The largest deviations in thrombin occur near the poorly defined C-terminus of the A-chain. Thus, thrombin essentially accommodates fragment 2 complex formation with little change in its folded structure. The rms difference in the Cα positions of thrombin between HF2– and BF2–thrombin is only 0.3 and 0.2 Å if 91 differences $>1\sigma$ are not considered. Interestingly, the largest difference (0.75 Å) occurs at His57, and the next largest difference is only 0.5 Å. Therefore, species difference in F2 also does not affect the structure of thrombin.

From the sequences of HF2 and BF2 (Figure 1), the A- and C-loops have a fairly high degree of conservation (15 of 31, 50%), but the same is not so for the B- and D-loops (9 of 38, 24%). This is also generally true of kringle modules found in other protein systems (Tulinsky et al., 1988b). Moreover, the lengths of the loops of the F1 and F2 kringles are identical.

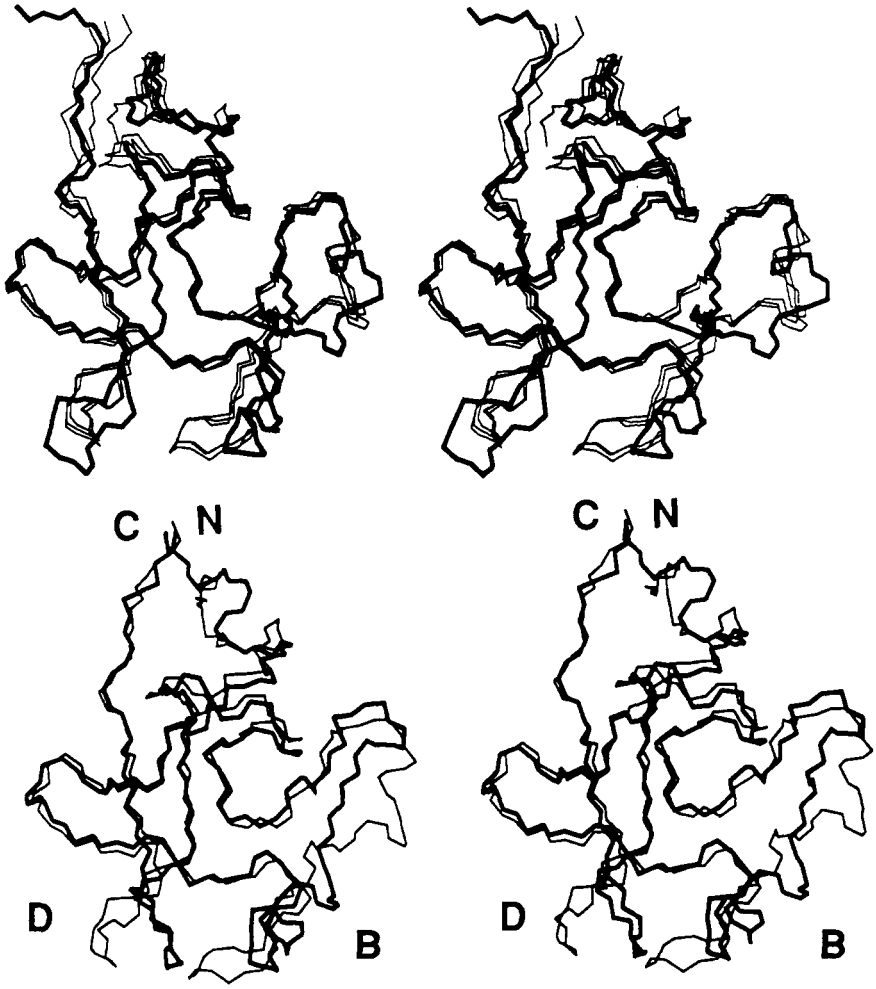

FIGURE 7: Stereoview comparing the CαCN folding of kringles. (Top) Prothrombin K1, plasminogen K1 and K4, and TPA K2. TPA K2 is shown in bold. (Bottom) Kringles 1 and 2 of prothrombin. Kringle 2 of HF2 is shown in bold.

Since the folding of kringle 1 of F1 (Seshadri et al., 1991), plasminogen kringle 1 (unpublished results of this laboratory) and kringle 4 (Mulichak et al., 1991) is the same (Figure 7, top), it is somewhat surprising that the folding of kringle 2 in HF2- and BF2-thrombin differs from these kringles (Figure 7, bottom). Kringle 2 of TPA also has a different folding (Byeon & Llinas, 1991; de Vos et al., 1992) (Figure 7, top), but this has been attributed to its different-sized loop structure.

The folding between HF2 and BF2 differs at Glu307–Glu310 (~1.2 Å) and Ser341–Ala342 (0.9 Å) but is virtually the same elsewhere (rms = 0.5 and 0.3 Å without 23 differences $>1\sigma$); the former difference in the first folded loop of the kringle is adjacent to a glycosylation site in prothrombin kringle 1 (Figure 1). The folding of HF2 is compared with kringle 1 of F1 in Figure 7 (bottom), from which it can be seen that the second outer B-loop assumes a completely different conformation with a distorted two-turn helix (Ala328–Lys335) and the hairpin β-turn of the second inner loop pivots as a unit about 60° at Val364 and Asp370. These features lead to 30 interdomain contacts less than 4.0 Å (Table V), which appear to be as important as the electrostatic interaction in maintaining the structures of the complexes. The β-turn region of TPA kringle 2 is also different from K1 of F1 (Figure 7, top), showing a greater twist of the β-strand compared to plasminogen kringles 1 and 4; however, it does not have a hinged pivot motion as found in HF2–thrombin (Figure 8). The movement in HF2 and BF2 is most likely a kringle conformational change accompanying complexation, *revealing a new flexibility aspect heretofore unobserved in kringles*, which is different, in principle, from the multiple utilization of the lysine binding site displayed by the thrombin complexes and the binding of a heparin-like fragment by the kringle of urokinase (Stephens et al., 1992). Binding of a lysine-like ligand (ACA) in the lysine binding site of plasminogen K4 (Wu et al., 1991) or TPA K2 (Byeon & Llinas, 1991) has little effect on the native structure. Residues Gly369–Asp370 of kringle 2 run parallel to Tyr94–Asn95 of thrombin at about 3.5–4.0 Å, and in the bovine complex Pro368 is sandwiched in between Ile90 and Pro92.

Except for the foregoing conformational difference in F2, and the generally differently folded B-loop, the folding of the F1 and F2 kringles is practically the same within the error of their determination. This is especially the case for the first inner loop (Figure 9), which comprises the anionic center of lysine-binding kringles that produces the principal electrostatic interaction with thrombin in the HF2 complex, making 18 contacts less than 4.0 Å with the putative heparin binding site (Table III). The same is not true of the region of HF2 corresponding to the cationic center of lysine-binding kringles, which neither possesses the requisite positively charged residues appropriately located nor the folding conformation of such kringles. The important positive residues in kringle 4 of plasminogen are Lys35 and Arg71 (position 70 in K1 of F1 and in F2) (Mulichak et al., 1991; Wu et al., 1991) and Lys33 in TPA kringle 2 (Byeon & Llinas, 1991; de Vos et al., 1992). In fragment 2, position 370 is aspartic acid and position 333 is leucine. Although Lys335 is conserved in both HF2 and BF2, it is on a turn of the helix of F2 which, as a consequence,

Table V: Interdomain Contacts <4.0 Å between Thrombin and the B- and D-Loops of HF2

thrombin	kringle	d (Å)	thrombin	kringle	d (Å)
Pro92CG	Leu333O	3.9	His91O	Pro368CB	3.2
Trp237CA	His336O	3.9	His91O	Pro368CG	4.0
Trp237CD1	His336O	3.4	Pro92CA	Pro368CB	3.9
Trp237CD1	His336CB	3.4	Pro92O	Pro368CA	3.4
Trp237NE1	His336CB	3.7	Pro92O	Pro368CB	3.6
Ala240CB	His336O	3.8	Pro92O	Pro368C	3.8
Ala240C	His336ND1	3.8	Trp96CD1	Pro368O	3.5
Ala240O	His336ND1	3.5	Trp96NE1	Pro368O	3.1 (H-bond?)
Pro92CB	Gln337NE2	3.7	Pro92O	Gly369N	3.0 (H-bond)
Pro92CG	Gln337NE2	3.3	Tyr94O	Gly369N	3.8
Pro92CB	Gln337NE2	3.7	Tyr94O	Gly369CA	3.2
Pro92CD	Gln337OE1	2.9	Arg97NE	Gly369O	3.1 (H-bond?)
			Arg97CZ	Gly369O	3.8
			Arg97NH2	Gly369O	3.6
			Arg97CZ	Asp370OD1	3.8
			Arg97NH2	Asp370CA	3.9
			Arg97NH2	Asp370CG	3.7
			Arg97NH2	Asp370OD1	2.5 (H-bond)

FIGURE 8: Stereoview comparing the CαCN folding of HF2 and TPA K2. HF2 is shown in bold.

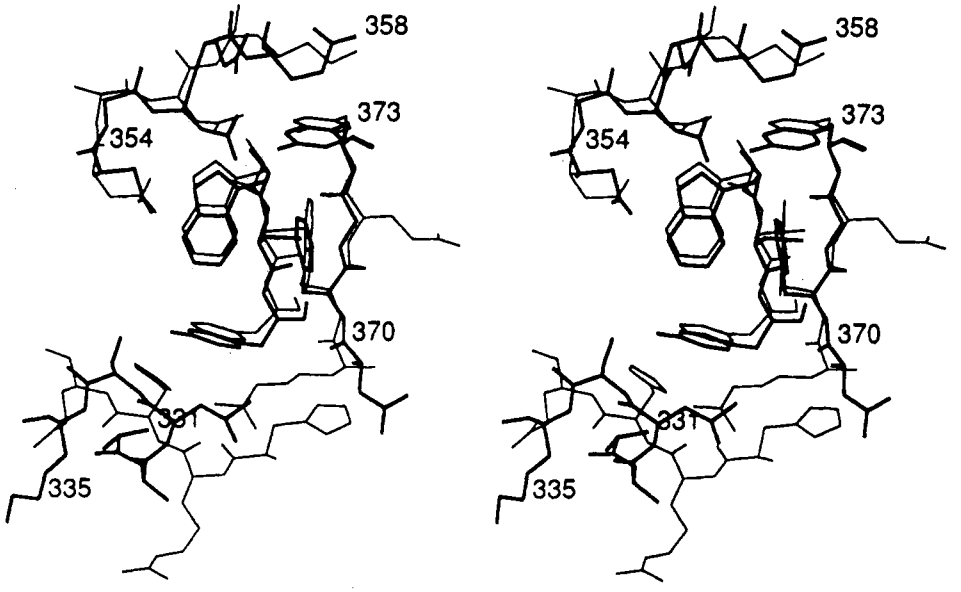

FIGURE 9: Stereoview comparing the lysine binding site of plasminogen kringle 4 with the same region in kringle 2 of F2. Kringle 2 is shown in bold; the anionic center of kringle 4 is at the top, and the cationic center is at the bottom.

causes it to project out into solvent, fatally disrupting any vestige of a cationic center.

The conformation of the second outer B-loop of the F2 kringle in the thrombin complex is different from that observed in all other kringles. Its most distinguishing characteristic is a distorted two-turn helix between Ala328 and Lys335 (Table VI). The kringle helical turns abut the Lys236–Val241 turn of the C-terminal helix of the B-chain of thrombin, possibly through an electrostatic interaction between Glu328 and Lys236/Lys240 in BF2, but which is Ala328 in HF2 (Figure

Table VI: Conformational Angles of Distorted Helical Turns in Kringle 2

	HF2		BF2	
residue	Φ (deg)	Ψ (deg)	Φ (deg)	Ψ (deg)
Ala328	−75	−43	−92	0
Gln329	−90	−29	−123	9
Ala330	−68	−4	−109	−10
Lys331	−100	−17	−98	−22
Ala332	−77	−57	−68	−72
Leu333	−56	−57	−46	−41
Ser334	−54	−8	−66	−16
Lys335	−70	−28	−76	−45

1). A helical turn also occurs in the same second outer loop of TPA kringle 2, but it is located five residues away between 41 and 45 (Byeon & Llinas, 1991; de Vos et al., 1992) (Figure 8) and is positionally very different three dimensionally from the helix of HF2. However, it is noteworthy that the kringle of urokinase, which has a much larger B-loop (Tulinsky et al., 1988b), possesses both of these helical structural features (Li et al., 1992). These three kringle structures reveal a folding flexibility that is inherent to kringles. It is also noteworthy that one of the differences between HF2 and BF2 occurs in the helical region. The remainder of the B-loop of HF2 is in an extended conformation that is again different from other kringles. Since the structure the F2 kringle alone has yet to be determined, it is not clear whether the different conformation of this loop is inherent to the kringle, as in TPA K2 and the urokinase kringle, or whether it might possibly be due to a conformational change upon complexation. In the latter case, the helical transition would seem to be induced by the close approach to the C-terminal helix of the B-chain of thrombin and its intense positive electrostatic field (Karshikov et al., 1992). However, since the F2 kringle could potentially display a lysine binding site if its folding corresponded to that of kringle 4, the fact that it is generally thought not to bind lysine is more consistent with it having a different native folding conformation. Further support for this inference is the observation by NMR that the same two-turn helix occurs in the urokinase kringle (Li et al., 1992). Lastly, the outer B-loop of the kringle makes one other impressive contact with thrombin, where His336 intercalates with Tyr89, Trp237, and Val241. Since this position is aspartate in bovine F2, its orientation is different.

The Active Site. The binding of BF2 has been shown to enhance esterolytic activity of both human and bovine α-thrombin, while that of HF2 does not (Myrmel et al., 1976). It has also been found to slow the rate of inhibition of thrombin by antithrombin III by inhibiting binding but not covalent complex formation (Walker & Esmon, 1979), to inhibit the clotting activity of thrombin, and to act as a competitive inhibitor of protein C activation (Jakubowski et al., 1986). More recently, such effects of F2 binding have been studied by observing fluorescence intensity changes of reporter groups bound to the active site of thrombin (Bock, 1992).

Although the active site is occupied by PPACK in the crystalline F2–thrombin complexes, the difference in response to HF2 and BF2 binding was probed by comparing the active site regions of the two complexes. The rms difference in atomic positions between the two is only 0.3 Å, which is well within the error of their determination. At the present relatively low resolution, the only significant difference between the two is in the position of His57. Otherwise, HF2 and BF2 have either no or the same effect on the active site when occupied by PPACK. Comparing the PPACK–thrombin structure with the active site of hirugen–thrombin (Skrzypczak-Jankun et al., 1991), which is unoccupied, shows some changes around His 57 and Asp189–Glu192 and a small movement in the vicinity of Trp60D. However, since the structures are at very different resolutions (2.2 Å for hirugen–thrombin), it is difficult to attach much significance to the differences. A more noteworthy difference between the complexes is the smaller number of interdomain interactions of BF2–thrombin. Even so, it is not clear how this difference may be related to the different responses observed upon HF2 and BF2 binding.

REFERENCES

Bajaj, S. P., Butkowski, R. J., & Mann, K. G. (1975) *J. Biol. Chem. 250*, 2150–2156.

Bloom, J. W., & Mann, K. G. (1978) *Biochemistry 17*, 4430–4438.

Bock, P. (1992) *J. Biol. Chem. 267*, 14974–14981.

Bode, W., Mayr, I., Baumann, U., Huber, R., Stone, S. R., & Hofsteenge, J. (1989) *EMBO J. 8*, 3467–3475.

Bode, W., Turk, D., & Karshikov, A. (1992) *Protein Sci. 1*, 426–471.

Brunger, A. T. (1990a) in *X-PLOR Manual (Version 2.1)*, Yale University, New Haven, CT.

Brunger, A. T. (1990b) *Acta Crystallogr. A46*, 46–57.

Brunger, A. T., Kuriyan, J., & Karplus, M. (1987) *Science 235*, 458–460.

Byeon, I. L., & Llinas, M. (1991) *J. Mol. Biol. 222*, 1035–1051.

Carter, C. W., Jr., & Carter, C. W. (1979) *J. Biol. Chem. 254*, 12219–12223.

Church, F. C., Pratt, C. W., Noyes, C. M., Kalayanamit, T., Sherril, G. B., Tobin, R. B., & Meade, B. (1989) *J. Biol. Chem. 264*, 18419–18425.

de Vos, A. M., Ultsch, M. H., Kelley, R. F., Padmanabhan, K., Tulinsky, A., Westbrook, M. L., & Kossiakoff, A. A. (1992) *Biochemistry 31*, 270–279.

Dombrose, F. A., Gitel, S. N., Zawalich, K., & Jackson, C. M. (1979) *J. Biol. Chem. 254*, 5027–5040.

Elion, J., Boissel, J.-P., Bonniec, B. L., Bezeaud, A., Jandrot-Perrus, M., Rabiet, M.-J., & Guillin, M.-C. (1986) *Bioregulatory Functions of Thrombin* (Walz, D. A., Fenton, J. W., II, & Shuman, M. A., Eds.) pp 16–26, New York Academy of Sciences, New York.

Esmon, C. T., & Jackson, C. M. (1974) *J. Biol. Chem. 249*, 7791–7797.

Fenton, J. W., II (1986) *Ann. N.Y. Acad. Sci. 485*, 5–15.

Finzel, B. C. (1987) *J. Appl. Crystallogr. 20*, 53–55.

Fitzgerald, P. A. M. (1988) *J. Appl. Crystallogr. 21*, 273–278.

Hewett-Emmett, D., McCoy, L. E., Hassouna, H. I., Reuterby, J., Walz, D. A., & Seegers, W. H. (1974) *Thromb. Res. 5*, 421–427.

Howard, A. J., Gilliland, G. L., Finzel, B. C., Poulos, T. L., Ohlendorf, D. H., & Salemme, F. R. (1987) *J. Appl. Crystallogr. 20*, 383–387.

Jakubowski, H. V., Kline, M. D., & Owen, W. G. (1986) *J. Biol. Chem. 261*, 3876–3882.

Karshikov, A., Bode, W., Tulinsky, A., & Stone, S. R. (1992) *Protein Sci. 1*, 727–735.

Lee, B., & Richards, F. M. (1971) *J. Mol. Biol. 55*, 379–400.

Lerch, P. G., Rickli, E. E., Lergier, W., & Gillesseu, D. (1980) *Eur. J. Biochem. 107*, 7–13.

Li, X., Smith, R. A. G., & Dobson, C. M. (1992) *Biochemistry 31*, 9562–9571.

Liu, L.-W., Ye, J., Johnson, A. E., & Esmon, C. T. (1991) *J. Biol. Chem. 266*, 23632–23636.

Magnusson, S., Petersen, T. E., Sottrup-Jensen, L., & Claeys, H. (1975) *Proteases and Biological Control* (Reich, E., Rifkin, D. B., & Shaw, E., Eds.) pp 123–149, Cold Spring Harbor Laboratory, Cold Spring Harbor, NY.

Mann, K. G. (1987) *Trends Biochem Sci. 12*, 229–233.

McLean, J. W., Tomlinson, J. E., Juang, W. J., Eaton, D. L., Fless, E. Y., Scanu, A. M., & Lawn, R. M. (1987) *Nature 330*, 132–137.

Mulichak, A. M., Tulinsky, A., & Ravichandran, K. G. (1991) *Biochemistry 30*, 10576–10588.

Myrmel, K. H., Lundblad, R. L., & Mann, K. G. (1976) *Biochemistry 15*, 1767–1773.

Nelsestuen, G. L. (1976) *J. Biol. Chem. 251*, 5648–5656.

Nesheim, M., Hibbard, L. S., Tracy, P. B., Bloom, J. W., Myrmel, K. H., & Mann, K. G. (1980) *The Regulation of Coagulation* (Mann, K. G., & Taylor, F. R., Eds.) pp 145–149, Elsevier North-Holland, Inc., New York.

Padmanabhan, K., Padmanabhan, K. P., Tulinsky, A., Park, C. H., Bode, W., Huber, R., Blankenship, D. T., Cardin, A. D., & Kisiel, W. (1993) *J. Mol. Biol.* (in press).

Park, C. H., & Tulinsky, A. (1986) *Biochemistry 25*, 3977–3983.

Patthy, L. (1985) *Cell 41*, 657–663.

Prendergast, F. G., & Mann, K. G. (1977) *J. Biol. Chem. 252*, 840–850.

Qiu, X., Padmanabhan, K. P., Carperos, V. E., Tulinsky, A., Kline, T., Maraganore, J. M., & Fenton, J. W., II (1992) *Biochemistry 31*, 11689–11697.

Rydel, T. J., Ravichandran, K. G., Tulinsky, A., Bode, W., Huber, R., Reitsch, C., & Fenton, J. W., II (1990) *Science 249*, 277–280.

Rydel, T. J., Tulinsky, A., Bode, W., & Huber, R. (1991) *J. Mol. Biol. 221*, 583–601.

Seshadri, T. P., Tulinsky, A., Skrzypczak-Jankun, E., & Park, C. H. (1991) *J. Mol. Biol. 220*, 481–494.

Skrzypczak-Jankun, E., Carperos, V. E., Ravichandran, K. G., Tulinsky, A., Westbrook, M., & Maraganore, J. M. (1991) *J. Mol. Biol. 221*, 1379–1393.

Soriano-Garcia, M., Padmanabhan, K., deVos, A. M., & Tulinsky, A. (1992) *Biochemistry 31*, 2554–2566.

Stenflo, J. (1974) *Proc. Natl. Acad. Sci. U.S.A. 71*, 2730–2733.

Stephens, R. W., Bokman, A. M., Myohanen, H. T., Reisberg, T., Tapiovaara, H., Pedersen, N., Grondahl-Hansen, J., Llinas, M., & Vaheri, A. (1992) *Biochemistry 31*, 7572–7579.

Trexler, M., Vali, Z., & Patthy, L. (1982) *J. Biol. Chem. 257*, 7401–7406.

Tulinsky, A. (1991) *Thromb. Haemostasis 66* (1), 16–31.

Tulinsky, A., & Qiu, X. (1993) *Blood Coagulation Fibrinolysis* (in press).

Tulinsky, A., Park, C. H., Mao, B., & Llinas, M. (1988a) *Proteins 3*, 85–96.

Tulinsky, A., Skrzypczak-Jankun, E., & Park, C. H. (1988b) *J. Mol. Biol. 202*, 885–901.

Vali, Z., & Patthy, L. (1984) *J. Biol. Chem. 259*, 13690–13694.

Walker, F. J., & Esmon, C. T. (1979) *J. Biol. Chem. 254*, 5618–5622.

Wu, T. P., Padmanabhan, K., Tulinsky, A., & Mulichak, A. (1991) *Biochemistry 30*, 10589–10594.